Heat and Mass Transfer (2020) 56:1453–1462
https://doi.org/10.1007/s00231-019-02764-1

ORIGINAL

Investigation of the influences of kaolin-deionized water nanofluid on the thermal behavior of concentric type heat exchanger

Ataollah Khanlari[1] · Duygu Yılmaz Aydın[2] · Adnan Sözen[3] · Metin Gürü[2] · Halil İbrahim Variyenli[3]

Received: 30 May 2019 / Accepted: 9 October 2019 / Published online: 13 December 2019

Abstract

Different strategies have been proposed to improve the efficiency of the energy conversion systems. One of the outstanding technics for heat transfer increment is utilizing nanofluid as working fluid. This experimental study investigates the effect of using kaolin/deionized water nanofluid that is comprise various kinds of metal oxides in different ratios, on thermal behavior of counter flow concentric tube (CFCT) heat exchanger and parallel flow concentric tube (PFCT) heat exchanger. The prepared kaolin/deionized water nanofluid solution has 2% (wt/wt) nanoparticle concentration. Also, to prevent flocculation and to enhance stability of the prepared nanofluid, sodium dodecyl benzene sulfonate surface-active agent has been mixed into the solution. The experiments have been conducted in various conditions to investigate the influence of using nanofluid. Utilizing kaolin/deionized water nanofluid as working fluid caused maximum improvement of 37% and 12% in overall heat transfer coefficient in CFCT and PFCT heat exchangers respectively, in comparison with deionized water.

Nomenclature

A	heat transfer area (m^2)
c_p	specific heat capacity (kJ/kg.K)
C	heat capacity rate (W/K)
$\dot{E}_{loss}$	exergy loss (W)
e	dimensionless exergy loss
h	heat transfer coefficient ($W/m^2.K$)
lpm	liter per minute
$\dot{m}$	mass flow rate (kg/s)
$\dot{Q}$	heat transfer rate (W)
s	specific entropy (J/kg.K)
T	temperature (K)
ΔT_{ln}	logarithmic mean temperature difference (K)
U	overall heat transfer coefficient ($W/m^2.K$)
W_R	total uncertainty (%)
w_1, w_2, w_n	the uncertainties in the independent variables
ε	effectiveness

Subcrips

i	inner
o	outer
R	the function uncertainty
T	total

1 Introduction

In the last years, increasing world population led to rise in global energy demand. Therefore, efficient energy conversion systems gain importance because of limited fossil resources and also increasing greenhouse gas emissions. In addition, one of the crucial issues is effective heat transfer that perform by heat exchangers [1, 2]. Several kinds of heat exchangers are utilized in various industries. Moreover, different strategies were utilized to upgrade the thermal performance of the heat exchangers. One of outstanding techniques is mixing nanoparticles into working fluid in order to enhance the thermal performance [3–7]. In this regard metallic or non-metallic nanoparticles is added to a base fluid like water. Nanoparticles has higher thermal conductivity in comparison with the base fluid. Therefore, adding nanoparticles to the base fluid improves thermal conductivity of working fluid by increasing thermal transfer surface area. Also, by using nanoparticles effective thermal capacity of the fluid increases. Additionally, nanoparticles lead to increase in fluid activity and turbulence intensity which is the main parameter that

✉ Ataollah Khanlari
akhanlari@thk.edu.tr; ata_khanlari@yahoo.com

[1] Faculty of Engineering, Department of Mechanical Engineering, University of Turkish Aeronautical Association, Ankara, Turkey

[2] Faculty of Engineering, Department of Chemical Engineering, Gazi University, Ankara, Turkey

[3] Faculty of Technology, Department of Energy Systems Engineering, Gazi University, Ankara, Turkey

affect thermal conductivity of nanofluid. The physical facts that mentioned above are the main reasons which cause to improve in the heat transfer by using nanofluids [8, 9]. Nanoparticle size, shape and its concentration are the most crucial parameters that influence nanofluid properties [10, 11]. Various nanofluids have been investigated by many researchers in the literature. The utilization of ZnO/water in plate type heat exchanger conducted by Kumar et al. [12]. Their results indicated that corrugation angle of heat exchanger affect the nanofluid thermal performance. Huang et al. analyzed impact of using hybrid type nanofluid including carbon nanotubes and Al_2O_3 on thermal performance [13]. Their findings indicated that using this hybrid nanofluid had not significant effect on heat transfer enhancement. Sözen et al. tested alumina and fly ash nanofluids performance in concentric tube type heat exchanger in two different mode. The findings illustrated that fly ash nanofluid improved the efficiency of heat exchanger more than alumina nanofluid [14].

The impact of nanoparticle ratio on thermal characteristics of nanofluid have been investigated in different studies. Tiwari et al. examined the impact of particle ratio on performance of four various nanofluids comprising CeO_2/water, Al_2O_3/water, SiO_2/water, and TiO_2/water. Their findings exhibited that the optimal nanoparticle ratio belongs to nanoparticle material, base fluid, and working conditions [15]. Gürü et al. tested the impact of particle ratio on thermal behavior of bentonite-water nanofluid in the heat pipe. Their findings illustrated a maximum increment of 37% in the heat pipe efficiency [16]. Also, the properties of surfactant is important which is used to avoid sedimentation in the nanofluid solution. Sözen et al. analyzed the influence of utilizing two various surfactants on the performance of TiO_2/water in the heat pipe. The experimental findings indicated that using sodium dodecyl benzene sulfonate surfactant was more effective than Triton X-100 [17].

Table 1 summarize some studies that used different nanofluid in various heat exchangers. Generally, in the literature studies metal oxides like TiO_2, Fe_2O_3, Al_2O_3 and SiO_2 were used separately to prepare nanofluid. In this study kaolin nanoparticles has been used to prepare nanofluid solution. The major goal of this study is to predict thermal characteristics of kaolin/deionized water nanofluid in CFCT and PFCT heat exchangers. Unlike conventional nanofluids which are prepared from one metal oxide, kaolin mainly consists of Al_2O_3, SiO_2, TiO_2 components together. The most significant feature that separates this work from the available research is that kaolin/deionized water nanofluid has been made by utilizing kaolin nanoparticles in optimal dimension and particle concentration with surface active agent utilization to avoid deposition and sedimentation issues.

2 Material and methods

2.1 Experimental apparatus

Schematic of the test apparatus which was utilized in this study is presented in Fig. 1. Two fluid loops are available in the test apparatus consists of hot and cold fluid loops. Hot fluid (nanofluid) is heated by two electrical heaters in the hot fluid tank and is circulated in hot fluid loop. In the experimental setup to monitor the fluid level a bullseye has been placed. Circuit breakers have been placed in the setup to prevent unexpected temperature jump in the hot fluid tank. Also, a pressure regulator has been added against the unexpected jump in pressure. To adjust flow rate in each fluid loop, two flow meters have been mounted to the system. As it is clear in Fig. 1 ten thermocouples have been located in different positions to monitor temperature in cold and hot sides. The technical specifications of the equipment which were utilized in the experimental apparatus are presented in Table 2. In the heat exchanger part of the experimental apparatus, hot fluid (nanofluid) passes over the interior tube, however cold fluid (water) passes over the external tube of heat exchanger. Flexible design of the test setup permits to counter flow and also parallel flow heat exchange. In parallel flow heat exchanger mode, valve number 1–4 were kept open but valve numbers 5–7 were closed. However, among counter flow heat exchanger mode of the experimental apparatus valve numbers 1, 4, 5, 6 and 7 were left open, but valve numbers 2 and 3 were closed (Fig. 1). Hot fuild is heated by electrical heaters in the hot fluid tank and then is transmitted to the heat exchanger part by means of a circulation pump. Hot fluid passes over interior tube of heat exchanger and release its thermal energy and return to the hot fluid tank. However, cold fluid passes over the exterior tube of heat exchanger and absorbs the heat which released by hot fluid and then is drained form the system.

2.2 Preparation of the nanofluid

First of all, to reduce kaolin particles' size and to obtain uniform nanoparticles ball milling process, using Spex-8000, has been applied for 8 h. In the second step, kaolin nanoparticles has been mixed into deionized water as the base fluid. The prepared nanofluid solution has 2% (wt/wt) particle content. Moreover, to prevent flocculation and to enhance stability of the nanofluid, sodium dodecyl benzene sulfonate surface-active agent has been added to the solution. Adding surface-active agent increases wetting capability of the nanofluid solution and reduces surface tension. Finally, nanofluid solution has been subjected to continuous pulsing by utilizing ultrasonic bath with the aim of enhancing stability of the prepared nanofluid.

Many types of nanoparticles do not have toxic effects [25], yet nanoparticles are used in bio applications widely environmentally friendly [26] and some of them have beneficial health effects [27]. Clays are non-toxic nanoparticles. Kaolin is a type of clay found in nature. Kaolin is used in health care products, as a filler and coating in paper industry, as a pesticide in agriculture, an adsorbent and a filter material [28–30]. Kaolin waste can also be used as building material. For example, they are used as cement in green concrete mixing [31]. Utilized kaolin in this study is taken from nature. There is no harm to the environment.

Density of kaolin/deionized water nanofluid has been determined by taking weight of a specified volume of nanofluid solution at the ambient temperature by utilizing analytical balance (Radwag AS220 CZ). Viscosity of the prepared nanofluid is other significant characteristics that must be determined. The viscosity of the kaolin/deionized water nanofluid has been determined in different temperatures using viscometer device (AND SV-10). In addition, nanofluid's heat capacity has been achieved by utilizing Differential Scanning Calorimetry (DSC) technic. In this regard Perkin Elmer Diamond DSC apparatus has been utilized to determine kaolin/deionized water nanofluid's heat capacity.

2.3 Experimental procedure

In the first step of the experiments in hot loop of the heat exchanger water has been tested as working fluid. Secondly, prepared kaolin/deionized water nanofluid has been utilized in hot fluid loop of experimental setup to determine its thermal performance. The experiments have been performed at 13 various hot fluid flow rates to analyze the effect of using nanofluid. However, flow rate of the cold fluid has been adjusted at 10 g/s. To obtain accurate findings every test has been iterated three times, then mean results have been utilized in the calculations.

2.4 Theoretical analysis

The amount of thermal energy which transferred in a heating system can be expressed as the gained thermal energy by cold side ($\dot{Q}_{cold}$) or the thermal energy released from the hot side ($\dot{Q}_{hot}$). The thermal energy which transferred from the hot side could be calculated as:

$$\dot{Q}_{hot} = \dot{m}_{hot}.c_{p,hot}.(T_3 - T_6) \quad (1)$$

Also, the absorbed thermal energy by the cold side is defined as below:

$$\dot{Q}_{cold} = \dot{m}_{cold}.c_{p,cold}.(T_7 - T_{10}) \quad (2)$$

It should be indicated that the mean value of specific heat capacity has been used in the calculations.

The highest efficiency can be obtained where the heat transfer in the hot side is the same with heat transfer in the cold side by supposing; the heat transfer from interior pipe (hot side) to exterior pipe (cold side), neglecting thermal resistance of heat transfer surface, and also ignoring measurement errors:

$$\dot{Q}_{hot} = \dot{Q}_{cold} \quad (3)$$

The convection heat transfer among pipe surface and working fluid during heat transfer across the pipe could be obtained as:

$$\dot{Q} = h\,A\,\Delta T_{ln} \quad (4)$$

here h denotes the heat transfer coefficient (HTC) among working fluid and the interior surface of exchanger pipe, A

Table 1 Some available researches related to nanofluid utilization in different systems

Reference	Nanofluid	Heat exchanger	Particle ratio (%)	Particle dimension (nm)	Findings
Duangthongsuk and Wongwises [18]	TiO_2/water	Double tube	0.2% vol.	21	HTC improved by 6–11%.
Pandey and Nema [19]	Al_2O_3/water	Plate type	2–4% vol.	40–50	4.6–10% improvement in HTC
Anoop et al. [20]	SiO_2/water	Plate type	2–6% wt.	20	Maximum 7% increment in HTC
Kabeel et al. [21]	Al_2O_3/water	Plate type	1–4% vol.	47	Maximum 13% improvement in HTC
Sun et al. [22]	Fe_2O_3/water, Cu/water and Al_2O_3/water	Plate type	0.1, 0.3, and 0.5%. wt.	50	Heat transfer rate significantly improved by increasing mass fraction of particles
Srinivas and Venu Vinod [23]	CuO/water TiO_2/water and Al_2O_3/water	Shell and helical coil	0.3, 0.6, 1, 1.5 and 2% wt.	10–40	Improvement in heat transfer rate
Özdemir and Ergun [24]	Al_2O_3/water	Plate type	2% wt.	100	16% increment in thermal efficiency

Fig. 1 Experimental setup

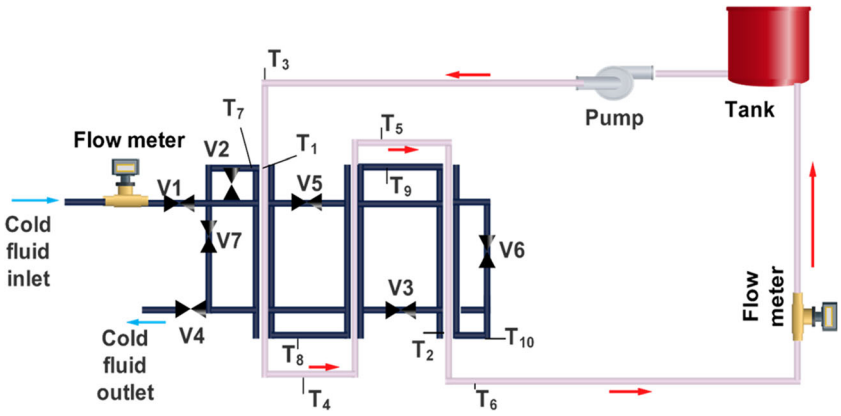

represents interior heat transfer surface area, and ΔT_{ln} illustrate logarithmic mean temperature difference and calculated as:

$$\Delta T_{ln} = \frac{\Delta T_{inlet} - \Delta T_{outlet}}{\ln\left(\frac{\Delta T_{inlet}}{\Delta T_{outlet}}\right)} \tag{5}$$

By rearranging equations above heat removed from the hot side can be calculated as:

$$\dot{Q}_{hot} = \frac{h_{hot}\, A_i\, [(T_3 - T_1) - (T_6 - T_2)]}{\ln\left(\frac{T_3 - T_1}{T_6 - T_2}\right)} \tag{6}$$

HTC in the hot side could be obtained by utilizing Eq. (6). In addition, heat transfer rate in the cold side of system is obtained by using Eq. (7).

Table 2 Technical specifications of the equipment which were utilized in the test apparatus

Equipment	Properties/capacity
Pump head (mSS)	1.5
Heat source (kW)	1.5
Flow meter of cold side (g/s)	4–50
Flow meter of hot side (g/s)	0.016–0.167
Types of thermocouple	J
Temperature indicator's sensitivity (°C)	0.1
Hot side interior radius (mm)	3.95
Hot side exterior radius (mm)	4.75
Cold side interior radius (mm)	5.55
Cold side exterior radius (mm)	6.35
Interior heat transfer surface (mm^2)	26,000
Exterior heat transfer surface (mm^2)	31,000
Heat transfer surface surface (mm^2)	28,800
Total flow surface area (m^2)	49×10^{-6}

$$\dot{Q}_{cold} = \frac{h_{cold}\, A_o\, [(T_1 - T_7) - (T_2 - T_{10})]}{\ln\left(\frac{T_1 - T_7}{T_2 - T_{10}}\right)} \tag{7}$$

In addition, heat transfer rate can be calculated using Eq. (8). By using Eq. (8) overall heat transfer coefficient (OHTC) in heat exchanger could be obtained [14].

$$\dot{Q}_{hot} = A_T\, U \left[\frac{(T_3 - T_7) - (T_6 - 10)}{\ln\left(\frac{T_3 - T_7}{T_6 - 10}\right)}\right] \tag{8}$$

Heat exchanger effectiveness can be achieved by using the Eq. (9):

$$\varepsilon = \frac{\dot{Q}}{\dot{Q}_{max}} = \frac{C_{hot}\left(T_{hot,i} - T_{hot,o}\right)}{C_{min}\left(T_{hot,i} - T_{cold,i}\right)} = \frac{C_{cold}\left(T_{cold,o} - T_{cold,i}\right)}{C_{min}\left(T_{hot,i} - T_{cold,i}\right)} \tag{9}$$

where the cold fluid heat capacity rate (C_{cold}) and the hot fluid heat capacity rate (C_{hot}) are:

$$C_{hot} = \dot{m}_{hot}\, c_{p,hot} \tag{10}$$

$$C_{cold} = \dot{m}_{cold}\, c_{p,cold} \tag{11}$$

Exergy could be defined as the maximum quantity of work achieved theoretically at the end of a reversible procedure in

Table. 3 Properties of measurement equipment

Device	Specifications	Uncertainty
Temperature measuring device	J-Type, measurement range (0–350 °C) Device accuracy: 0.5 °C	±0.588 °C
Flow meters	Cold fluid, measurement range 4–50 (g/s) Hot fluid, measurement range 1–10 (lpm) Device accuracy: ±5 (%)	±5.36% ±5.13%

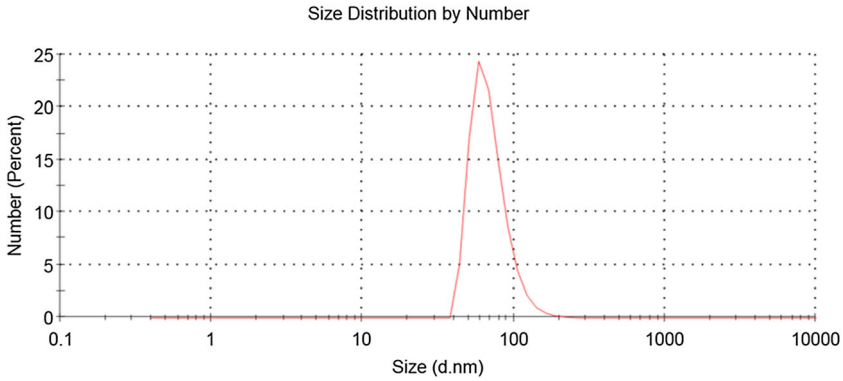

Fig. 2 Kaolin nanoparticles' size distribution

that equilibrium with the environment is acquired. In regard to this description, the reference environment conditions should be identified to calculate exergy. In the present work reference environment temperature is 22 °C. In a heat exchanger there are two types of losses including; frictional pressure drop and temperature difference. But in this work, exergy analysis dose not consist pressure drop factor and has been done according to heat transfer irreversibility. Therefore, exergy loss in the heat exchanger is the sum of exergy losses of cold and hot flows [32, 33]:

$$\dot{E}_{loss} = \dot{E}_{loss,hot} + \dot{E}_{loss,cold} \tag{12}$$

Eq. (12) can be rewritten as:

$$\dot{E}_{loss} = \dot{m}_{hot} T_e \left(s_{hot,o} - s_{hot,i}\right) + \dot{m}_{cold} T_e \left(s_{cold,o} - s_{cold,i}\right) \tag{13}$$

By supposing constant thermophysical properties for the fluids, entropy change can be expressed as:

$$s_o - s_i = c_p \ln \frac{T_o}{T_i} \tag{14}$$

Therefore, Eq. (13) can be rewritten as follow:

$$\dot{E}_{loss} = T_e \dot{m}_{hot} c_p ln\left(\frac{T_{hot,o}}{T_{hot,i}}\right) + T_e \dot{m}_{cold} c_p ln\left(\frac{T_{cold,o}}{T_{cold,i}}\right) \tag{15}$$

By considering a base for the fluid with maximum temperature range, i.e. the fluid with minimum heat capacity rate, dimensionless exergy loss for the heat exchanger could be obtained as:

$$e = \frac{\dot{E}_{loss}}{T_e C_{min}} \tag{16}$$

Table 4 Kaolin particles chemical content (%) and loss on ignition (LOI)

SiO_2	Al_2O_3	K_2O	CaO	TiO_2	MgO	Fe_2O_3	Na_2O	LOI
48.2	38.1	1.2	1.06	0.99	0.9	0.5	0.09	8

where C_{min} denotes minimum heat capacity rate and T_e shows ambient temperature.

2.5 Experimental uncertainty

Among the experimental process, temperatures and flow rates have been achieved by utilizing proper measurement. Uncertainty analysis is a useful technique to obtain uncertainties and to appraise the experimental findings. The uncertainties could arise from device selecting, calibration of device, reading, experimental conditions, and connection types of devices [34]. The properties of utilized equipment during experiments and their uncertainty including relative flow rate uncertainty and absolute temperature uncertainty were given in Table 3. The accuracy of wattmeter, flow meter and thermocouples are ±1 W, ±0.01 g/s and 0.5 °C, respectively. Total relative uncertainty in temperature measurement is 2%. Also, uncertainty for heat transfer coefficient obtained as 6.4%. As it is obvious, the obtained results for uncertainty, are in acceptable range by considering sensitivity of utilized devices and available studies in literature [35, 36].

$$W_R = \left[\left(\frac{\partial R}{\partial x_1} w_1\right)^2 + \left(\frac{\partial R}{\partial x_2} w_2\right)^2 + \ldots + \left(\frac{\partial R}{\partial x_n} w_n\right)^2\right]^{1/2} \tag{17}$$

Table 5 Thermophysical specifications of kaolin/deionized water nanofluid

Working fluid	Viscosity (mPa s)				Density (kg/m^3)	Specific heat capacity (kJ/kgK)
	20 (°C)	40 (°C)	60 (°C)	80 (°C)		
Deionized water	0.98	0.64	0.45	0.35	998	4.18
Kaolin/deionized water	1.03	0.94	0.71	0.57	1012	4.34

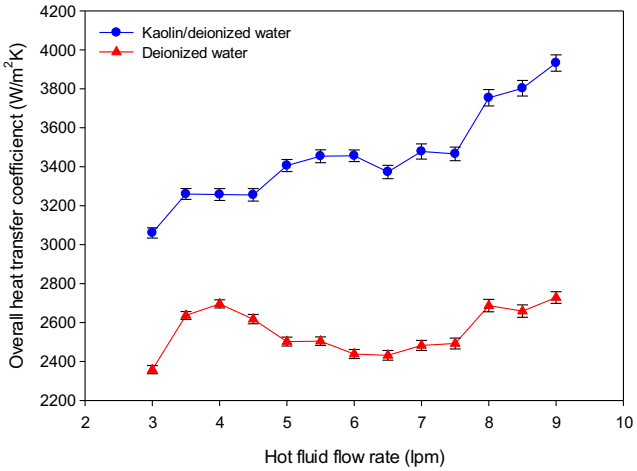

Fig. 3 OHTC variation via hot fluid flow rate in PFCT heat exchanger

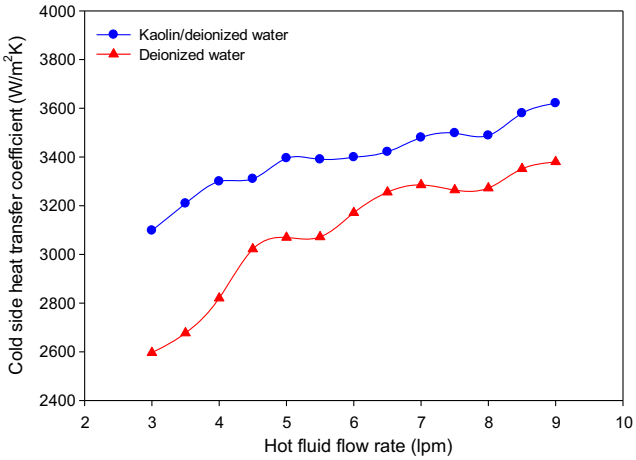

Fig. 5 HTC of cold side via hot fluid flow rate in PFCT heat exchanger

3 Results and discussion

In this part, the experimental findings for both CFCT and PFCT heat exchangers are given and the obtained results are concluded. An average size of 69 nm has been obtained for kaolin nanoparticles at the end of ball milling process. Size distribution for the kaolin nanoparticles is presented in Fig. 2. Chemical composition of kaolin nanoparticles is given in Table 4. Also, the thermophysical specifications of kaolin/deionized nanofluid are given in Table 5.

The experiments have been performed at constant cold side flow rate (10 g/s) and 13 different hot fluid (nanofluid) flow rates to clarify the influence of utilizing nanofluid in hot fluid loop.

The variation of OHTC via hot fluid (nanofluid) flow in PFCT heat exchanger for deionized water and nanofluid is presented in Fig. 3. As it is obvious, OHTC of kaolin/deionized water nanofluid is high in comparison with deionized water at each hot fluid flow rate. A peak enhancement of 37% was achieved at 7 lpm flow rate by using kaolin/deionized water. The experimental findings illustrated that utilizing kaolin/deionized water in hot loop of the heat exchanger caused to increment in OHTC.

The change in the HTC of hot fluid among the interior surface of tube and the hot fluid via hot fluid flow rate in PFCT heat exchanger is presented in Fig. 4. The obtained HTC of kaolin/deionized water nanofluid is high in comparison with deionized water's HTC at each flow rate, with a maximum increment of 39%. As it is seen in Fig. 4 hot fluid (nanofluid) heat transfer coefficient improved by rising hot fluid flow rate for nanofluid and deionized water.

The change in HTC of cold fluid with flow rate of hot fluid in PFCT heat exchanger is presented in Fig. 5. The obtained cold side HTC for kaolin/deionized water nanofluid is high in comparison with deionized water at each flow rate, with a peak enhancement of 19%. In addition, it should be stated that HTC of cold fluid improved by rising with hot fluid flow rate for each working fluid.

The change in of OHTC via flow rate of hot fluid (nanofluid) in CFCT heat exchanger for both deionized water and kaolin/deionized water nanofluid is presented in Fig. 6.

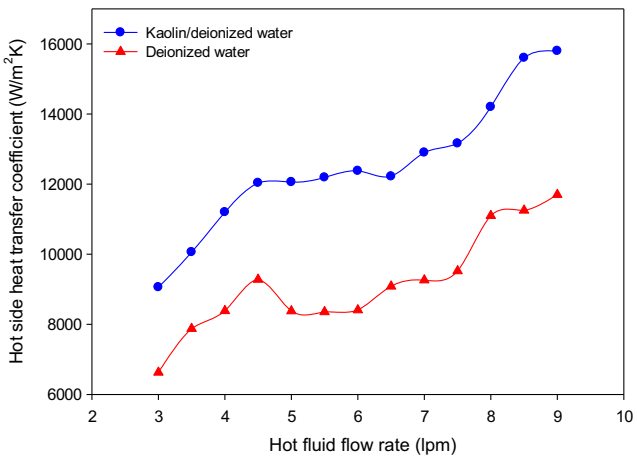

Fig. 4 HTC of hot side via hot fluid flow rate in PFCT heat exchanger

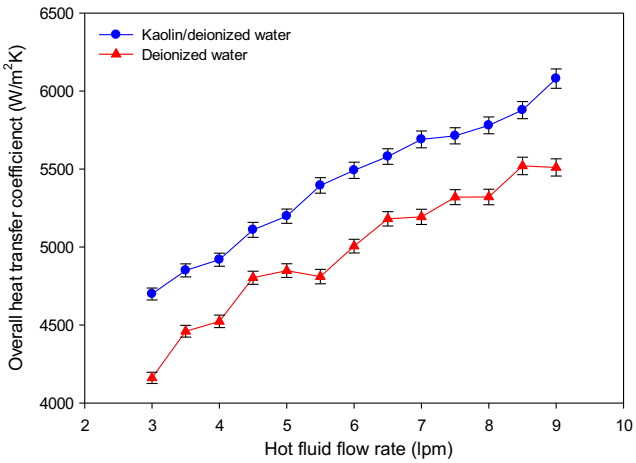

Fig. 6 OHTC variation via hot fluid flow rate in CFCT heat exchanger

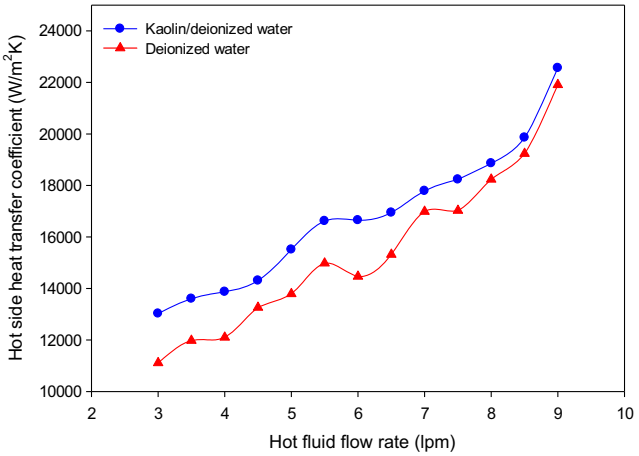

Fig. 7 HTC of hot side via hot fluid flow rate in CFCT heat exchanger

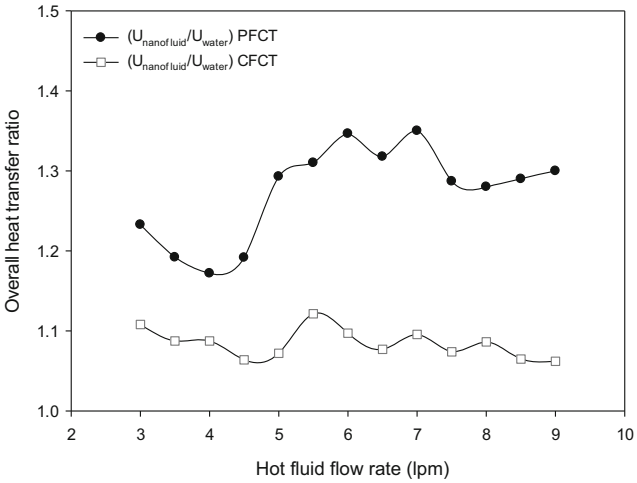

Fig. 9 OHTC ratio via hot fluid flow rate

The OHTC of kaolin/deionized water nanofluid is high in comparison with deionized water for each flow rate of hot fluid. A maximum increment of 12% was obtained for kaolin/deionized water nanofluid at 5.5 lpm flow rate. The achieved findings illustrated that using kaolin/deionized water in hot loop of the CFCT heat exchanger led to enhance in thermal performance of CFCT heat exchanger.

The change in the hot fluid HTC among interior surface of exchanger tube and hot fluid via hot fluid flow in CFCT heat exchanger is presented in Fig. 7. The HTC of the kaolin/deionized water nanofluid is high in comparison with deionized water at each flow rate of hot fluid, with a maximum enhancement of 15%. As it can be seen in Fig. 7 HTC in hot side improved by rising hot fluid flow rate for both nanofluid and deionized water.

The variation of HTC in cold side among the exterior area of exchanger tube and cold fluid via hot fluid flow rate in CFCT heat exchanger is presented in Fig. 8. The achieved cold side HTC for kaolin/deionized water is higher than deionized water at each flow rate, with a peak enhancement of 9%. Also, it should be stated that cold fluid heat transfer coefficient improved by rising hot fluid flow rate for both working fluids.

The variation in the OHTC ratio ($U_{nanofluid}/U_{deionized\ water}$) via hot side flow rate for two heat exchangers is shown in Fig. 9. In the PFCT heat exchanger, OHTC ratio varied in a range of 1.17–1.35 in various hot fluid flow rates. Also, OHTC ratio for CFCT heat exchanger changed in a range of 1.07–1.12. Variation of hot side HTC ratio ($h_{h,nanofluid}/h_{h,deionized\ water}$) via hot fluid flow rate for two heat exchangers is shown in Fig. 10. In PFCT heat exchanger, hot side HTC ratio varied in a range of 1.25–1.39 in various hot fluid flow rates. However, HTC ratio in hot side for CFCT heat exchanger changed in a range of 1.03–1.15. Variation of heat transfer coefficient ratio in cold side ($h_{c,nanofluid}/h_{c,deionized\ water}$) via hot fluid flow rate for both heat exchangers is presented in Fig. 11. In the PFCT heat exchanger, HTC ratio of cold side varied in a range of 1.07–1.19 in various hot fluid flow rates. However, HTC ratio in cold side for CFCT heat exchanger changed in a range of 1.04–1.09. The obtained results indicated that

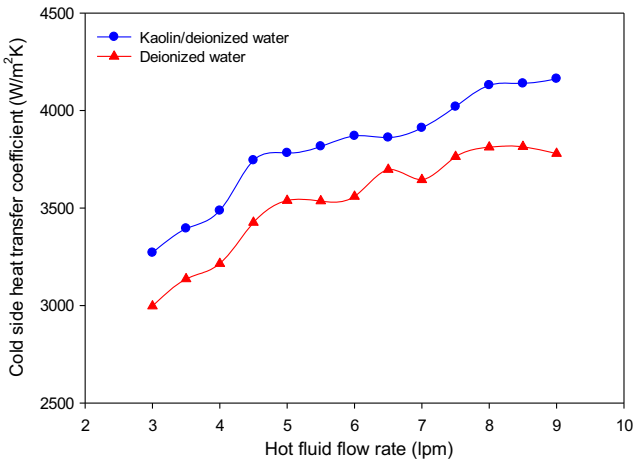

Fig. 8 HTC of cold side via hot fluid flow rate in CFCT heat exchanger

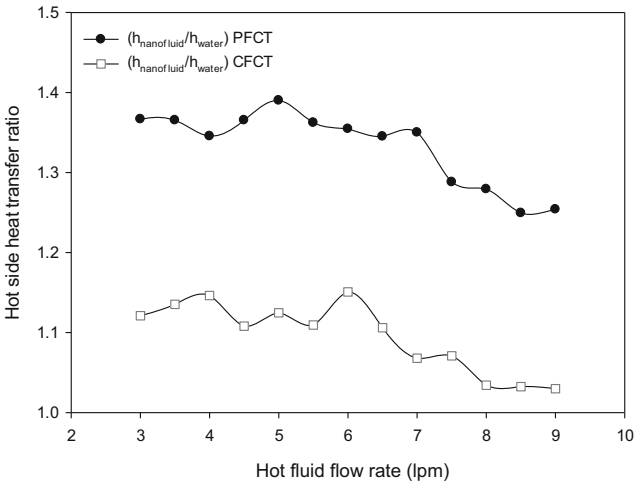

Fig. 10 Variation of hot fluid HTC ratio via hot fluid flow rate

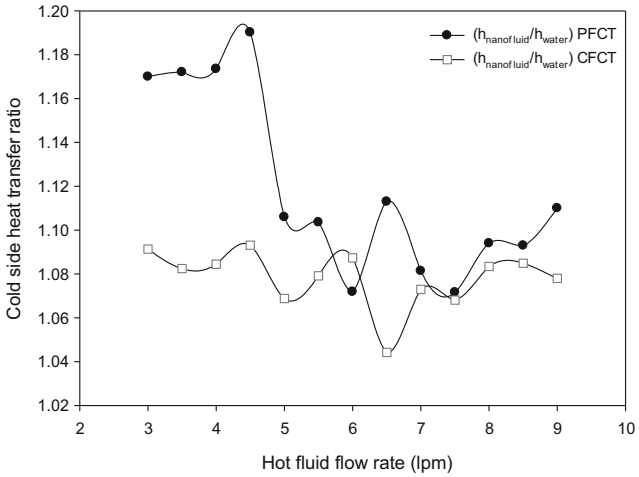

Fig. 11 Variation of cold fluid HTC ratio via hot fluid flow rate

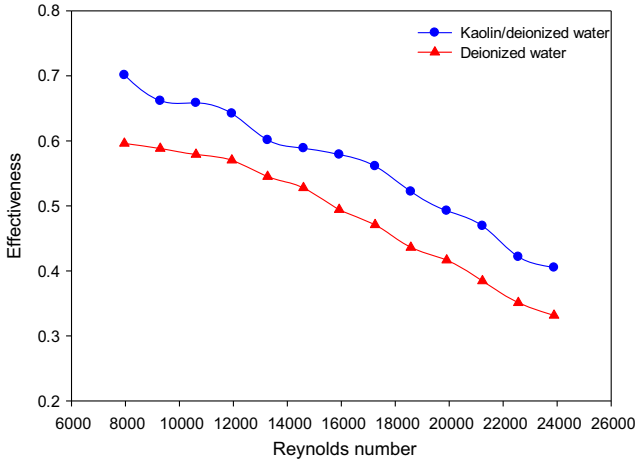

Fig. 13 Variation of effectiveness with Reynolds number for PFCT heat exchanger

increment in the performance of PFCT heat exchanger is high in comparison with CFCT heat exchanger.

Moreover, Al_2O_3/water and fly ash/water nanofluids thermal behavior in concentric type heat exchanger was previously investigated by Sözen et al. [14, 37]. They tested nanofluids performance in ten different flow rates. Figure 12 presents a comparison between OHTC results for PFCT heat exchanger obtained in this study and previous studies. Sözen et al. reported maximum improvements of 62% and 7.2% for OHCT by using fly ash/water and Al_2O_3/water, respectively. However, in the present study a maximum improvement of 37% for OHTC was obtained by using Kaolin/ deionized water.

Variation of the effectiveness with Reynolds number for PFCT and CFCT heat exchangers are presented in Figs. 13 and 14. As it can be seen, utilizing Kaolin/deionized water increased the effectiveness PFCT and CFCT heat exchangers in the range of 7–20%. It is seen that effectiveness was decreased with increasing Reynolds number. As it is known Reynolds number increases with increasing fluid flow rate. Also, it should be stated that fluid heat capacity rate increases with increase in fluid flow rate, therefore temperature change of fluid decreases, which cause to reduce the effectiveness. In high flow rates, temperature variation will be lesser since fluid residual time is limited inside the heat exchanger and cause to decrease in effectiveness. Similar results for effectiveness of concentric type heat exchangers were obtained by Gomaa et al. [38, 39].

Variation of dimensionless exergy loss with Reynolds number for PFCT and CFCT heat exchangers are shown in Figs. 15 and 16. As it can be seen in figures, using Kaolin/deionized water reduced dimensionless exergy loss in PFCT and CFCT heat exchangers in the range of 18–39%. In addition, it should be stated that in CFCT heat exchanger the amount of heat transfer rate is higher in comparison to PFCT heat exchanger. Therefore, exergy loss in CFCT heat exchanger is lower

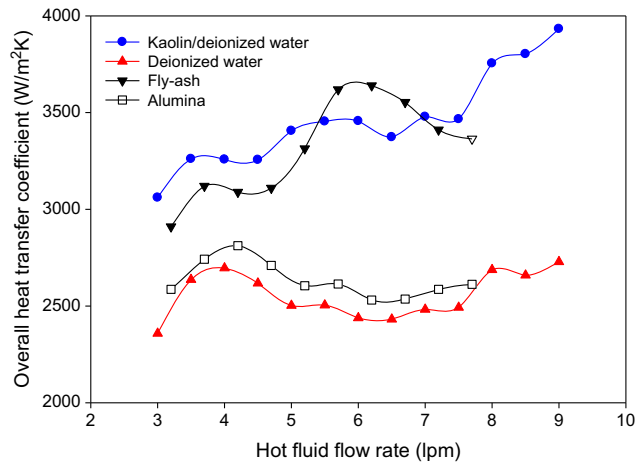

Fig. 12 Comparison between this study and previous studies

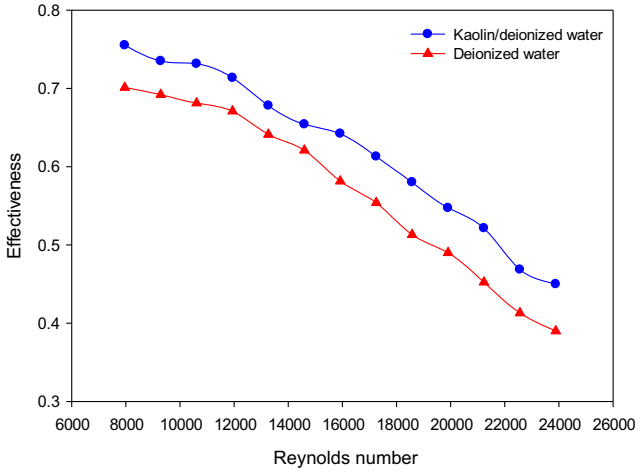

Fig. 14 Variation of effectiveness with Reynolds number for CFCT heat exchanger

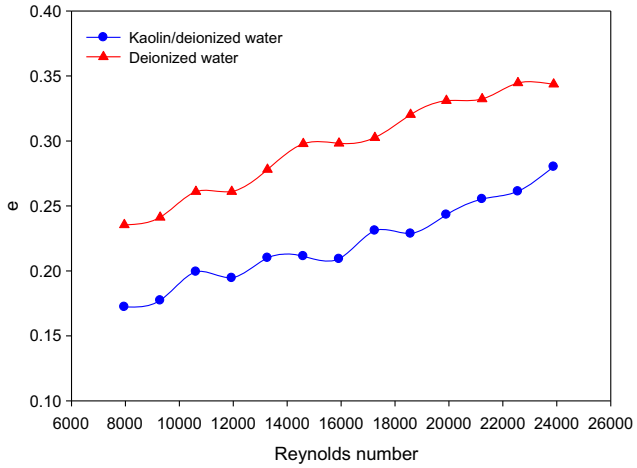

Fig. 15 Variation of dimensionless exergy loss with Reynolds number for PFCT heat exchanger

in comparison with PFCT heat exchanger. This fact illustrates once again that, more exergy loss in heat exchanger is not directly related to the heat transfer rate. The significant factor which affect exergy loss is finite temperature difference among cold and hot water in heat exchanger. Therefore, it must be avoided high local temperature difference among hot and cold fluid over the heat exchanger.

Outcomes of the experiments exhibited that, using kaolin/deionized water in the hot side of the PFCT and CFCT heat exchangers improved heat transfer performance considerably. Also, it should be stated that the viscosity of kaolin/deionized water is relatively close to the viscosity of water (see Table 5). Therefore, utilizing kaolin/deionized water nanofluid don't cause to pressure drop in the heat exchangers.

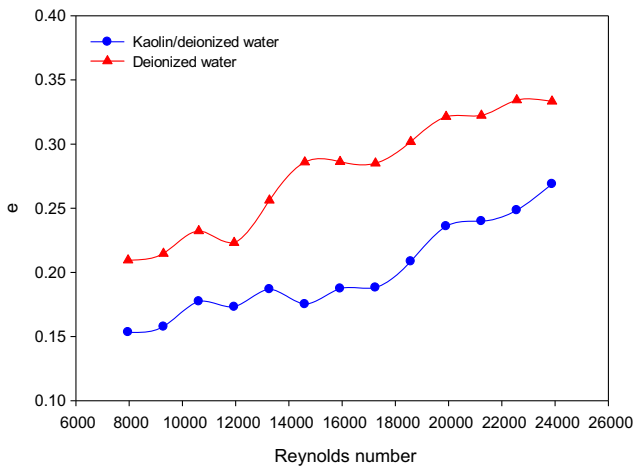

Fig. 16 Variation of dimensionless exergy loss with Reynolds number for CFCT heat exchanger

4 Conclusions

In the present study the impact of utilizing kaolin/deionized water nanofluid on the thermal efficiency of two different heat exchanger including PFCT and CFCT heat exchangers have been investigated. The experiments have been conducted in different working conditions to determine thermal behavior of kaolin/deionized water. Utilizing kaolin/deionized water nanofluid in the PFCT and CFCT heat exchangers improved heat transfer performance considerably. Maximum improvement in the OHTC in PFCT and CFCT heat exchangers were obtained as 37% and 12%, respectively. The experimental findings exhibited that kaolin/deionized water could be utilized effectively in the concentric tube type heat exchanger. Moreover, kaolin/deionized water's thermal behavior in various energy conversion systems can be analyzed.

Compliance with ethical standards

Conflict of interest On behalf of all authors, the corresponding author states that there is no conflict of interest.

References

1. Afshari F, Comakli O, Lesani A, Karagoz S (2017) Characterization of lubricating oil effects on the performance of reciprocating compressors in air-water heat pumps. Int J Refrig 74:503–514
2. Afshari F, Comakli O, Karagoz S, Ghasemi Zavaragh H (2018) A thermodynamic comparison between heat pump and refrigeration device using several refrigerants. Energ Buildings 168:272–283
3. Menlik T, Sözen A, Gürü M, Öztaş S (2015) Heat transfer enhancement using MgO/water nanofluid in heat pipe. J Energy Inst 88: 247–257
4. Khanları A, Sözen A, Variyenli Hİ (2018) Simulation and experimental analysis of heat transfer characteristics in the plate type heat exchangers using TiO_2/water Nanofluid. Int J Numer Methods Heat Fluid Flow 29(4):1343–1362
5. Ağbulut Ü, Sarıdemir S (2018) A general view to converting fossil fuels to cleaner energy source by adding nanoparticles. Int J Ambient Energ. https://doi.org/10.1080/01430750.2018.1563822
6. Barzegarian R, Keshavarz Moraveji M, Aloueyan A (2016) Experimental investigation on heat transfer characteristics and pressure drop of BPHE (brazed plate heat exchanger) using TiO_2–water nanofluid. Exp Thermal Fluid Sci 74:11–18
7. Barzegariana R, Aloueyanb A, Yousef T (2017) Thermal performance augmentation using water based Al_2O_3-gamma nanofluid in a horizontal shell and tube heat exchanger under forced circulation. Int Commun Heat Mass Transfer 86:52–59
8. Kaya M, Gürel AE, Ağbulut Ü, Ceylan I, Çelik S, Ergün A, Acar B (2019) Performance analysis of using CuO-methanol nanofluid in a hybrid system with concentrated air collector and vacuum tube heat pipe. Energy Convers Manag 199:111936. https://doi.org/10.1016/j.enconman.2019.111936
9. Sözen A, Gürü M, Khanlari A, Çiftçi E (2019) Experimental and numerical study on enhancement of heat transfer characteristics of a heat pipe utilizing aqueous clinoptilolite nanofluid. Appl Therm Eng 160:114001. https://doi.org/10.1016/j.applthermaleng.2019.114001

10. Avramenko AA, Shevchuk IV, Tyrinov AI, Blinov DG (2014) Heat transfer at film condensation of stationary vapor with nanoparticles near a vertical plate. Appl Therm Eng 73:389–396
11. Avramenko AA, Shevchuk IV, Moskalenko AA, Lohvynenko PN, Kovetska YY (2018) Instability of a vapor layer on a vertical surface at presence of nanoparticles. Appl Therm Eng 139:87–98
12. Kumar V, Tiwari AK, Kumar Ghosh S (2016) Effect of chevron angle on heat transfer performance in plate heat exchanger using ZnO/water nanofluid. Energy Convers Manag 118:142–154
13. Huang D, Wu Z, Sunden B (2016) Effects of hybrid nanofluid mixture in plate heat exchangers. Exp Thermal Fluid Sci 72:190–196
14. Sözen A, Variyenli Hİ, Özdemir MB, Gürü M, Aytaç I (2016) Heat transfer enhancement using alumina and fly ash nanofluids in parallel and cross-flow concentric tube heat exchangers. J Energy Inst 89:414–424
15. Tiwari AK, Ghosh P, Sarkar J (2015) Particle concentration levels of various nanofluids in plate heat exchanger for best performance. Int J Heat Mass Transf 89:1110–1118
16. Gürü M, Sözen A, Karakaya U, Çiftçi E (2019) Influences of bentonite-deionized water nanofluid utilization at different concentrations on heat pipe performance: an experimental study. Appl Therm Eng 148:632–640
17. Sözen A, Gürü M, Menlik T, Karakaya U, Çiftçi E (2018) Experimental comparison of Triton X-100 and sodium dodecyl benzene sulfonate surfactants on thermal performance of TiO_2–deionized water nanofluid in a thermosiphon. Experimental Heat Transfer 31:450–469
18. Duangthongsuk W, Wongwises S (2008) Effect of thermophysical properties models on the predicting of the convective heat transfer coefficient for low concentration nanofluid. Int Commun Heat Mass Transfer 35:1320–1326
19. Pandey SD, Nema VK (2012) Experimental analysis of heat transfer and friction factor of nanofluid as a coolant in a corrugated plate heat exchanger. Exp Thermal Fluid Sci 38:248–256
20. Anoop K, Cox J, Sadr R (2013) Thermal evaluation of nanofluids in heat exchangers. Int Commun Heat Mass Transfer 49:5–9
21. Kabeel AE, El Maaty TA, El Samadony Y (2013) The effect of using nano-particles on corrugated plate heat exchanger performance. Appl Therm Eng 52:221–229
22. Sun B, Peng C, Zuo R, Yang D, Li H (2016) Investigation on the flow and convective heat transfer characteristics of nanofluids in the plate heat exchanger. Exp Thermal Fluid Sci 76:75–86
23. Srinivas T, Venu Vinod A (2016) Heat transfer intensification in a shell and helical coil heat exchanger using water-based nanofluids. Chem Eng Process Process Intensif 102:1–8
24. Özdemir MB, Ergun ME (2018) Experimental and numerical investigations of thermal performance of Al_2O_3/water nanofluid for a combi boiler with double heat exchangers. Int J Numer Methods Heat Fluid Flow 29(4):1300–1321
25. Das RK, Pachapur VL, Lonappan L, Naghdi M, Pulicharla R, Maiti S, Cledon M, Dalila LMA, Sarma SJ, Brar SK (2017) Biological synthesis of metallic nanoparticles: plants, animals and microbial aspects. Nanotechnol Environ Eng 2:18
26. Khan I, Saeed K, Khan I (2017) Nanoparticles: properties, applications and toxicities. Arab J Chem. https://doi.org/10.1016/j.arabjc.2017.05.011
27. Jeevanandam J, Barhoum A, Chan YS, Dufresne A, Danquah MK (2018) Review on nanoparticles and nanostructured materials: history, sources, toxicity and regulations. Beilstain J Nanotechnol 9:1050–1074
28. Ahmed NM (2013) Comparative study on the role of kaolin, calcined kaolin and chemically treated kaolin in alkyd-based paints for protection of steel. Pigm Resin Technol 42(1):3–14
29. Murray HH (1961) Industrial applications of kaolin. Clays Clay Miner 10:291–298
30. Viseras C, Aguzzi C, Cerezo P, Galindo AL (2007) Uses of clay minerals in semisolid health care and therapeutic products. Appl Clay Sci 36:37–50
31. Loty A, Karahan O, Ozbay E, Hossain KMA, Lachemi M (2015) Effect of kaolin waste content on the properties of normal-weight concretes. Constr Build Mater 83:102–107
32. Akpinar EK, Bicer Y (2005) Investigation of heat transfer and exergy loss in a concentric double pipe exchanger equipped with swirl generators. Int J Therm Sci 44:598–607
33. Heyhat MM, Abdi A, Jafarzad A (2018) Performance evaluation and exergy analysis of a double pipe heat exchanger under air bubble injection. Appl Therm Eng 143:582–593
34. Karagöz S, Afshari F, Yildirim O, Comakli O (2017) Experimental and numerical investigation of the cylindrical blade tube inserts effect on the heat transfer enhancement in the horizontal pipe exchangers. Heat Mass Transf 53:2769–2784
35. Tu YD, Wang RZ, Ge TS (2018) New concept of desiccant-enhanced heat pump. Energy Convers Manag 156:568–574
36. Afshari F, Karagoz S, Comakli O, Ghasemi Zavaragh H (2019) Thermodynamic analysis of a system converted from heat pump to refrigeration device. Heat Mass Transf 55(2):281–291
37. Sözen A, Variyenli Hİ, Özdemir MB, Gürü M (2016) Improving the thermal performance of parallel and cross-flow concentric tube heat exchangers using fly-ash nanofluid. Heat Transfer Eng 37:805–813
38. Gomaa A, Halim MA, Elsaid AM (2017) Enhancement of cooling characteristics and optimization of a triple concentric-tube heat exchanger with inserted ribs. Int J Therm Sci 120:106–120
39. Gomaa A, Halim MA, Elsaid AM (2016) Experimental and numerical investigations of a triple concentric-tube heat exchanger. Appl Therm Eng 99:1303–1315